Int. J. Electrochem. Sci., 17 **(2022)** Article Number: 220526, doi: 10.20964/2022.05.15

International Journal of
ELECTROCHEMICAL
SCIENCE
www.electrochemsci.org

Electrochemical Properties of UNS S 32750 and UNS S 32760 Annealed Super Duplex Stainless Steels

Changwon Sung [1], *Kyungchun Kim*[2], *Wonsub Chung*[3,*] *and Byung-Hyun Shin*[4,*]

[1] Kowel Corporation, Yangsan, Republic of Korea
[2] School of Mechanical Engineering, Pusan National University, Busan 46241, Republic of Korea
[3] School of Materials Science and Engineering, Pusan National University, Busan 46241, Republic of Korea
[4] Cold Rolling Production Engineering Team, Hyungdai steel, Dangjin-Si 31719, Republic of Korea
[*]E-mail: lemonhouse947@nate.com & wschung1@pusan.ac.kr

Received: 4 January 2022 / *Accepted:* 20 February 2022 / *Published:* 5 April 2022

Super duplex stainless steels (SDSSs) exhibit high pitting corrosion resistance in seawater because of their dual-phase composition of austenite and ferrite, requiring solution annealing. Therefore, the solution annealing (1100 °C) of SDSS is a crucial step to optimize the corrosion resistance of stainless steel during the manufacturing process. UNS S 32760 is an SDSS formed by adding 0.6 wt.% W and 0.7 wt.% Cu to UNS S 32750. The change in the chemical compositions of the alloys alters the solution annealing temperature. This study electrochemically analyzed the effects of the addition of Cu and W on the solution annealing of SDSS. UNS S 32750 and UNS S 32760 exhibited the most favorable electrochemical properties at 1100 and 1080 °C, respectively, owing to their chemical compositions. UNS S 32750 exhibited high pitting corrosion resistance, whereas UNS S 32760 exhibited highly uniform corrosion resistance.

Keywords: Electrochemical properties, Pitting corrosion, Critical pitting temperature, Solution annealing, Super duplex stainless steel.

1. INTRODUCTION

Structural materials used in offshore plants require high pitting corrosion resistance and strength [1, 2]. Although stainless steels generally exhibit high corrosion resistance, stainless steels comprising austenite or ferrite exhibit unfavorable pitting corrosion resistance [3, 4]. Conversely, duplex stainless steels exhibit high pitting corrosion resistance and strength [5–10]. The duplex stainless steels are classified into four groups based on the pitting resistance equivalent number (PREN; PREN = wt.% Cr

+ 3.3 wt.% Mo + 16 wt.% N) [1-4]. For super duplex stainless steels (SDSSs), the PREN is in the range 40–50.

SDSSs exhibit high uniform corrosion resistance, pitting corrosion resistance, and hydrogen embrittlement resistance [1, 2]. These electrochemical properties are affected by the heat-treatment conditions because of changes in the chemical composition due to changes in the volume fractions of austenite and ferrite [1-3]. Conventionally, SDSS UNS S 37250 is solution annealed at 1100 °C for the optimization of its electrochemical properties [11–19]. Because the chemical composition is affected by the solution annealing temperature, UNS S 32760 requires a specific solution annealing temperature.

Researchers have studied the effect of W on the mechanical properties of stainless steels [20–23]. Park et al. studied the effect of W on secondary phase precipitation in ferrite stainless steel (29 wt. % Cr) at 850 °C [12]. Ahn and Kang examined the effect of W and Mo on secondary phase precipitation in lea duplex stainless steel after heat treatment at 750 and 800 °C, respectively (PREN: 20–30) [18]. However, thus far, no study has investigated the effects of W and Cu on the electrochemical properties and solution annealing temperature of SDSS.

The most commonly used SDSS is UNS S 32750; UNS S 32760 was developed from UNS S 32750 by the addition of Cu and W to enhance the corrosion resistance of the original materials [18]. W and Cu are the body-centered cubic (BCC; ferrite) and face-centered cubic (FCC; austenite) stabilizer elements, respectively [12]. W improves pitting corrosion resistance, whereas Cu improves uniform corrosion resistance. However, changes in the chemical composition require to be studied in terms of the electrochemical properties and annealing conditions.

In this study, we investigated the electrochemical properties and solution annealing conditions of SDSS UNS S 32750 and UNS S 32760. The phase transformation as a function of the solution annealing temperature was examined using optical microscopy (OM) and field-emission scanning electron microscopy (FE-SEM). The chemical composition was determined using energy-dispersive X-ray spectroscopy (EDS). The electrochemical properties under different conditions were analyzed using potentiodynamic polarization curves, critical pitting temperature (CPT; potentiostatic test at 700 mV_{SCE}), and electrochemical impedance spectroscopy (EIS) measurements.

2. EXPERIMENTAL

The duplex stainless steel grade was determined based on the PREN (wt.% Cr + 3.3 wt.% Mo + 16 wt.% N). The SDSS (UNS S 32750 and UNS S 32760) used in this experiment had PREN in the range of 40–50 [3]. The materials were cast. Their chemical compositions are listed in Table 1.

Table 1. Chemical compositions of commercial SDSSs UNS S 32750 and UNS S 32760.

	C	**N**	**Mn**	**Ni**	**Cr**	**Mo**	**Cu**	**W**	**Fe**
UNS S 32750	0.01	0.27	0.8	6.8	25.0	3.8	0.2	0.02	Bal
UNS S 32760	0.01	0.24	0.6	6.7	25.2	3.7	0.7	0.60	Bal

The specimens were heat-treated from 950 °C (precipitation temperature of the secondary phase) to 1200 °C (ferritization temperature). A schematic is shown in Figure 1 [13].

This condition shows the effect of Cu and W as a function of the heat-treatment temperature. The effects of the heat treatment on the microstructure, volume fraction, and chemical composition were examined.

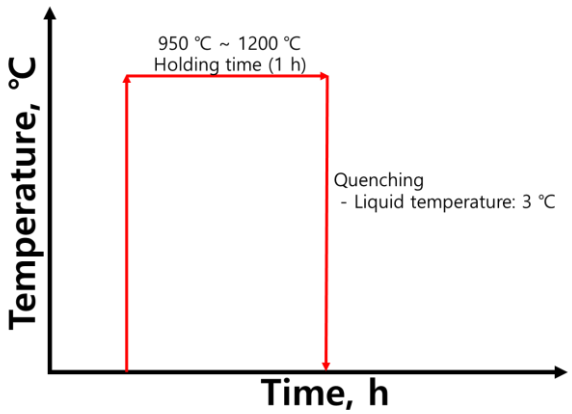

Figure 1. Schematic of heat-treatment (temperature 950–1200 °C; cooling method is quenching) of SDSSs UNS S 32750 and UNS S 32760.

The specimens subjected to microstructure and volume fraction analyses were etched at 5 V in a 20 wt.% NaOH solution after the surfaces were polished down to a diamond paste (particle diameter: 0.25 μm) [13]. The microstructures were analyzed by OM and FE-SEM. The volume fraction was calculated using an image analyzer, and the chemical composition was determined using EDS. However, the N composition calculated using EDS (interstitial elements) was inaccurate. Therefore, the N composition was calculated using the maximum solubility of ferrite with a volume fraction [1–5] according to the following formula:

$$N_r = \text{chemical composition of } N_{Total} \text{ wt. \%} - Ferrite_{VF} * 0.05 \text{ wt. \%},$$

where N_r is the chemical composition of N in austenite, and $Ferrite_{VF}$ indicates the volume fraction of ferrite.

The electrochemical properties of SDSS UNS S 32750 and UNS S 32760 were analyzed using potentiodynamic and potentiostatic tests. The potential vs. current density curve (potentiodynamic polarization test; analysis area: 1 cm2) expresses the change in the current density as a function of electrolyte (3.5 wt. % NaCl) potential from −0.5 V to 1.5 V; the scan rate was determined to be 0.167 mV. The reference and counter electrodes were a saturated calomel electrode (SCE) and a platinum mesh (dimensions: 20 × 20 mm), respectively. CPT and EIS analyses were conducted as potentiostatic tests. The CPT was determined in a 5.85 wt. % NaCl electrolyte at 700 mV. The CPT was determined as the temperature above a current density of over 100 μA/cm^2 for 60 s at a scan rate of 1 °C/min. EIS was

conducted from 10^{-1} Hz to 10^{7} Hz in a 3.5 wt. % NaCl electrolyte (Potential: 230 mV, current density 300 μA/cm^2).

3. RESULTS AND DISCUSSION

3.1. Microstructure as a function of the solution annealing temperature

The SDSS microstructure changes with the solution annealing condition [9-11]. Figures 2 and 3 show the UNS S 32750 and UNS S 32760 microstructures as functions of temperature ranging from 950 to 1150 °C.

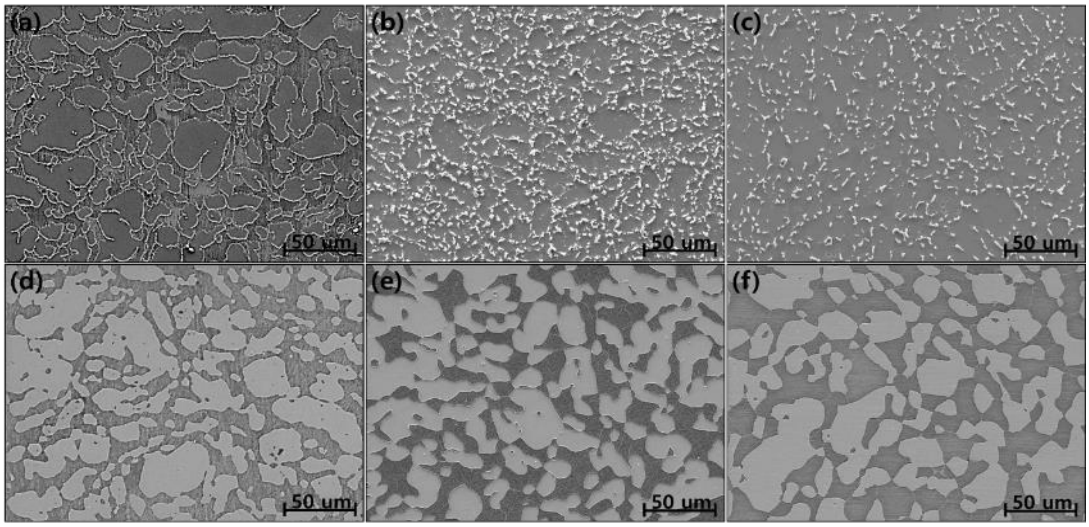

Figure 2. SDSS UNS S 32750 microstructure after etching in 20 wt. % NaOH with heat treatment: (a) casting, (b) 950 °C, (c) 1000 °C, (d) 1050 °C, (e) 1100 °C, and (f) 1150 °C.

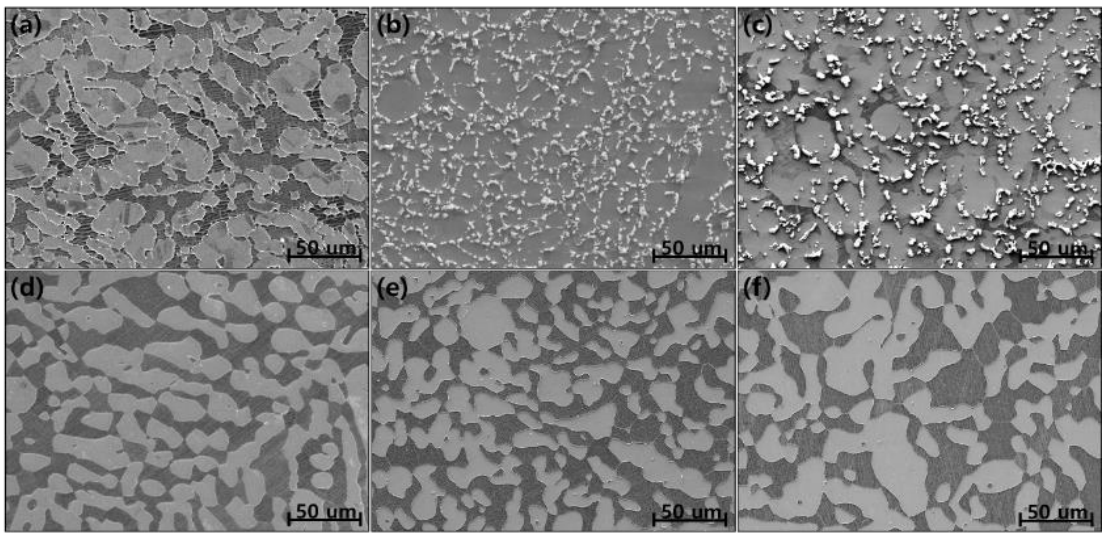

Figure 3. SDSS UNS S 32760 microstructure after etching in 20 wt. % NaOH with heat treatment: (a) casting, (b) 950 °C, (c) 1000 °C, (d) 1050 °C, (e) 1100 °C, and (f) 1150 °C.

The microstructure changes with heating temperature, and as shown in these figures, identical changes are observed at the same temperature for UNS S 32750 and UNS S 32760. Figure 4 shows the effects of Cu and W on the microstructure.

Figure 4 shows the microstructures of UNS S 32750 and UNS S 32760 after heat treatment at 1000 °C. The addition of Cu and W decreases the secondary phase precipitation. Figure 5 shows the effect on the volume fraction of the bare metal.

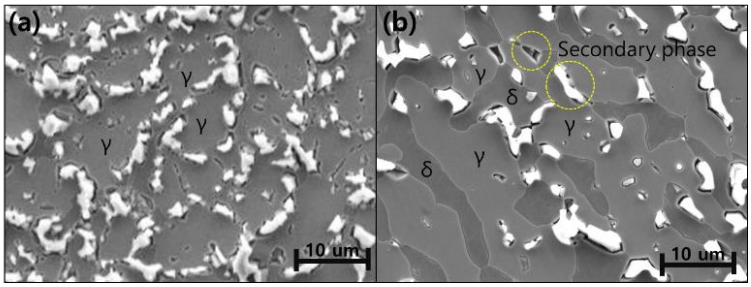

Figure 4. Microstructures of (a) UNS S 32750 and (b) UNS S 32760 with heat treatment at 1000 °C (precipitation temperature of secondary phase (Sigma & Chi)).

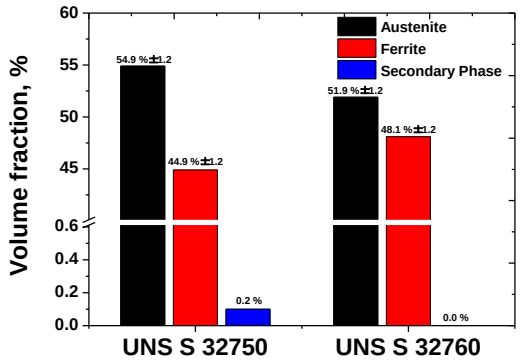

Figure 5. Volume fraction (austenite, ferrite, and secondary phase) of the cast UNS S 32750 and UNS S 32760.

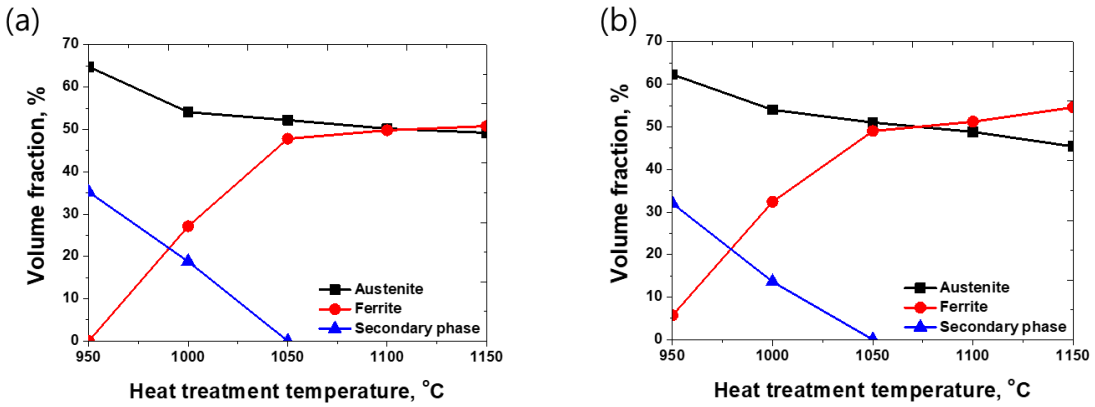

Figure 6. Volume fractions of (a) UNS S 32750 and (b) UNS S 32760 as functions of heat-treatment temperature.

The volume fraction of SDSS changes with the heat-treatment temperature [9, 10]. Figure 6 shows the volume fractions of UNS S 32750 and UNS S 32760 as functions of heat-treatment temperature. At the same temperature, UNS S 32760 exhibited a lower volume fraction of austenite than UNS S 32750.

Cu and W are the stabilization elements of austenite and ferrite, respectively. UNS S 32760 exhibited an increased volume fraction of ferrite at each temperature. The chemical compositions of UNS S 32750 and UNS S 32760 changed because of increases in the Cu and W compositions by 0.5 and 0.58 wt. %, respectively, consequently changing the volume fractions of UNS S 327560 and UNS S 32760. The volume fraction can be predicted using the Schaeffler diagram, and the Ni and Cr equivalents for calculating the coefficient are as follows [12]:

Ni equivalent: wt. % Ni + wt. % Co +30 wt. % C + 25 wt. % N + 0.5 wt. % Mn + 0.3 wt. % Cu.

Cr equivalent: wt.% Cr + 2 wt. % Si + 1.5 wt. % Mo + 5 wt. % V + 5.5 wt. % Al + 1.75 wt. % Nb + 1.5 wt. % Ti + 0.75 wt. % W.

We observed an increase in the volume fraction of ferrite greater than that of Cu by a factor of two at the same temperature. According to this equation, UNS S 32750 has a higher volume fraction of austenite than UNS S 32760 at the same temperature.

3.2. Chemical composition as a function of heat-treatment temperature

The change in the volume fraction of duplex stainless steel due to heat treatment affects its corrosion resistance because of the change in its chemical composition [23]. SDSS requires an equal PREN of austenite and ferrite to achieve the highest pitting corrosion resistance, because the low PREN phases of austenite and ferrite work at the pitting site [9]. Table 2 lists the chemical compositions as functions of heat-treatment temperature. Cr, Ni, Mo, Cu, and W were determined using EDS, whereas N was obtained from a previous study [5].

Table 2. Chemical compositions of (a) UNS S 32750 and (b) UNS S 32760 as a function of heat-treatment temperature.

(a)

Temperature (°C)	Phase	Cr	Ni	Mo	Cu	W	N
1030	Ferrite	27.4 ± 0.8	5.0 ± 0.5	5.3 ± 0.5	0.12 ± 0.0	0.03 ± 0.0	0.05
	Austenite	23.1 ± 0.9	8.1 ± 0.6	2.6 ± 0.3	0.23 ± 0.0	0.01 ± 0.0	0.44
1050	Ferrite	27.1 ± 0.8	5.2 ± 0.5	5.0 ± 0.5	0.12 ± 0.0	0.03 ± 0.0	0.05
	Austenite	23.1 ± 0.9	8.0 ± 0.6	2.7 ± 0.3	0.23 ± 0.0	0.01 ± 0.0	0.47
1080	Ferrite	26.8 ± 0.8	5.4 ± 0.5	4.6 ± 0.4	0.12 ± 0.0	0.03 ± 0.0	0.05
	Austenite	23.2 ± 0.8	7.9 ± 0.6	3.0 ± 0.3	0.23 ± 0.0	0.01 ± 0.0	0.49
1100	Ferrite	26.6 ± 0.8	5.5 ± 0.5	4.4 ± 0.4	0.20 ± 0.0	0.03 ± 0.0	0.05
	Austenite	23.3 ± 0.8	7.9 ± 0.6	3.2 ± 0.3	0.16 ± 0.0	0.01 ± 0.0	0.51
1150	Ferrite	26.5 ± 0.7	5.7 ± 0.6	4.4 ± 0.4	0.12 ± 0.0	0.03 ± 0.0	0.05

	Austenite	23.2 ± 0.9	7.7 ± 0.6	3.2 ± 0.3	0.24 ± 0.0	0.01 ± 0.0	0.54
1180	Ferrite	26.3 ± 0.9	6.0 ± 0.6	4.3 ± 0.4	0.12 ± 0.0	0.03 ± 0.0	0.05
	Austenite	23.3 ± 0.9	7.6 ± 0.6	3.2 ± 0.3	0.25 ± 0.0	0.01 ± 0.0	0.56
1200	Ferrite	26.1 ± 0.8	6.2 ± 0.6	4.3 ± 0.4	0.12 ± 0.0	0.03 ± 0.0	0.05
	Austenite	23.3 ± 0.9	7.5 ± 0.6	3.0 ± 0.3	0.28 ± 0.0	0.01 ± 0.0	0.62

(b)

Temperature (°C)	**Phase**	**Cr**	**Ni**	**Mo**	**Cu**	**W**	**N**
1030	Ferrite	27.7 ± 1.3	4.61 ± 0.5	5.19 ± 0.5	0.48 ± 0.0	0.79 ± 0.1	0.05
	Austenite	23.3 ± 1.2	8.34 ± 0.7	2.55 ± 0.3	0.89 ± 0.1	0.45 ± 0.0	0.44
1050	Ferrite	27.2 ± 0.8	4.86 ± 0.5	4.81 ± 0.5	0.50 ± 0.1	0.74 ± 0.1	0.05
	Austenite	23.5 ± 0.7	8.27 ± 0.7	2.77 ± 0.3	0.89 ± 0.1	0.48 ± 0.0	0.46
1080	Ferrite	26.6 ± 0.9	5.21 ± 0.5	4.39 ± 0.4	0.51 ± 0.1	0.74 ± 0.1	0.05
	Austenite	23.8 ± 0.9	8.16 ± 0.7	3.02 ± 0.3	0.91 ± 0.1	0.46 ± 0.0	0.49
1100	Ferrite	26.5 ± 0.6	5.4 ± 0.5	4.31 ± 0.4	0.51 ± 0.1	0.73 ± 0.1	0.05
	Austenite	23.9 ± 0.5	8.1 ± 0.7	3.07 ± 0.3	0.92 ± 0.1	0.46 ± 0.0	0.50
1150	Ferrite	26.2 ± 0.5	6.0 ± 0.5	4.21 ± 0.3	0.52 ± 0.1	0.72 ± 0.1	0.05
	Austenite	24.0 ± 0.5	7.6 ± 0.7	3.08 ± 0.3	0.94 ± 0.1	0.46 ± 0.0	0.53
1180	Ferrite	26.0 ± 0.7	6.1 ± 0.7	4.12 ± 0.3	0.52 ± 0.1	0.71 ± 0.1	0.05
	Austenite	24.2 ± 0.8	7.5 ± 0.7	3.16 ± 0.3	0.95 ± 0.1	0.46 ± 0.0	0.55
1200	Ferrite	25.9 ± 0.9	6.3 ± 0.7	4.01 ± 0.4	0.52 ± 0.1	0.71 ± 0.1	0.05
	Austenite	24.3 ± 1.0	7.4 ± 0.7	3.25 ± 0.3	0.99 ± 0.1	0.44 ± 0.0	0.59

The heat treatment affected the chemical composition, consequently changing the PREN, as shown in Figure 7.

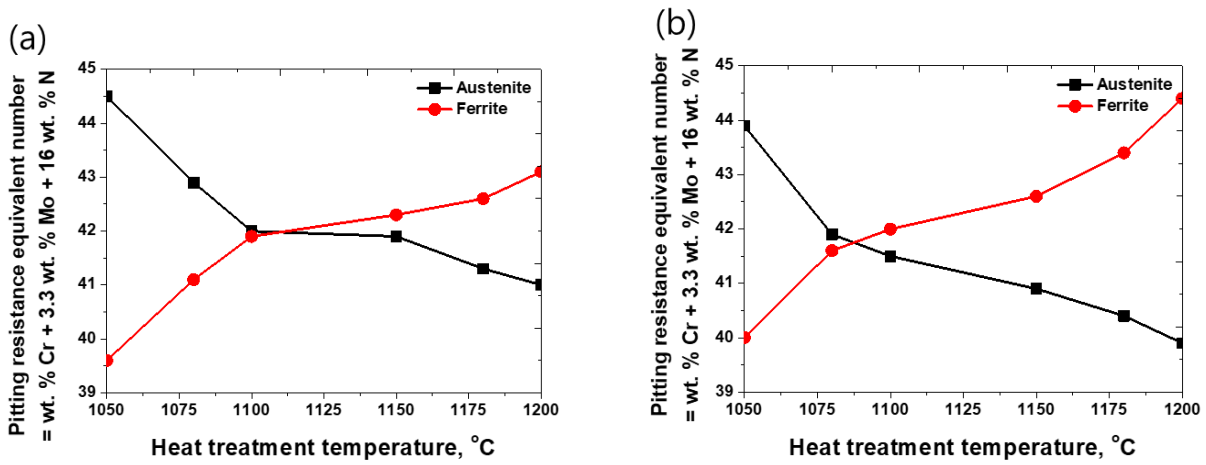

Figure 7. Figure 7. Pitting resistance equivalent number (PREN = wt. % Cr + 3.3 wt. % Mo + 16 wt. % N) of austenite and ferrite in (a) UNS S 32750 and (b) UNS S 32760, as functions of the heat-treatment temperature.

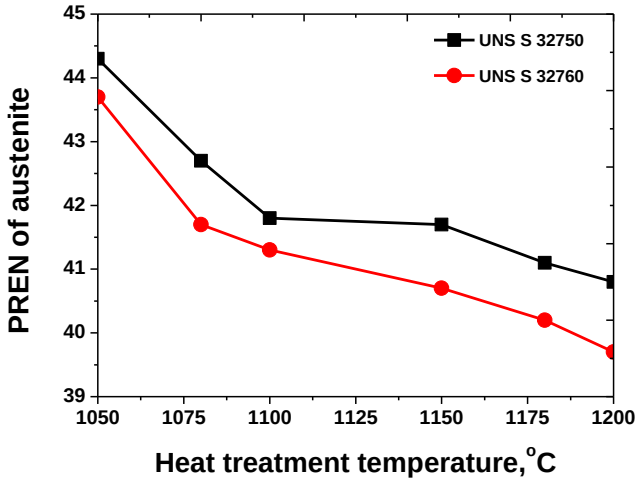

Figure 8. PREN of austenite in the SDSS as a function of heat-treatment temperature.

The change in PREN makes the cross point. The optimal heat-treatment temperatures for UNS S 32750 and UNS S 32760 are 1100 and 1080 °C, respectively. The volume fraction exhibits the same trend. As shown in Figure 8, UNS S 32760 consistently exhibits a lower PREN than UNS S 32750. This is attributable to W owing to the decrease in the volume fraction of ferrite.

3.3. Electrochemical properties as a function of heat-treatment temperature

The electrochemical properties of UNS S 32750 and UNS S 32760 were examined using the CPT, potentiodynamic polarization curves, and EIS analyses after solution annealing at 1100 °C.

As shown in Figure 9, the PREN affects the CPT. The highest CPT values for UNS S 32750 and UNS S 32760 were 1100 and 1080 °C, respectively. These results are similar to those of the volume fractions and PREN tendencies.

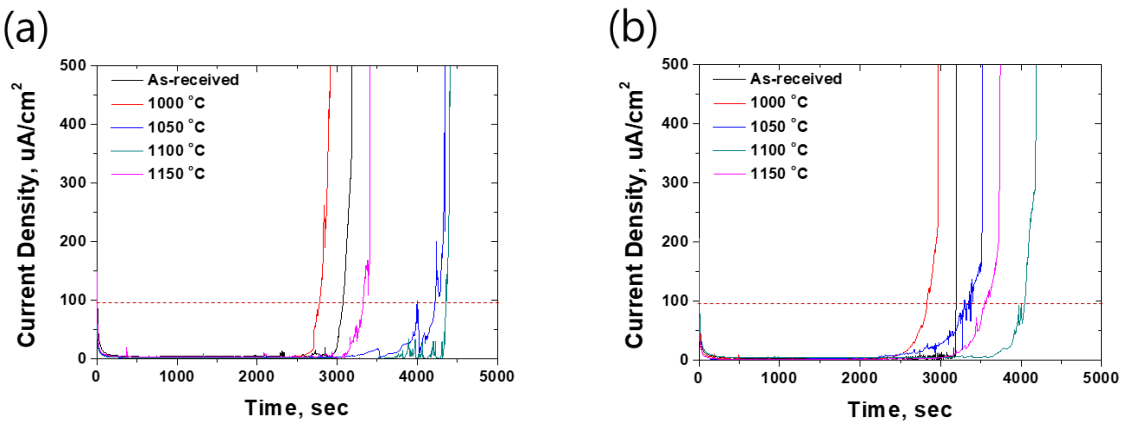

Figure 9. Critical pitting temperature as a function of heat-treatment temperature of SDSS at 700 mV in 5.85 wt. % NaCl.

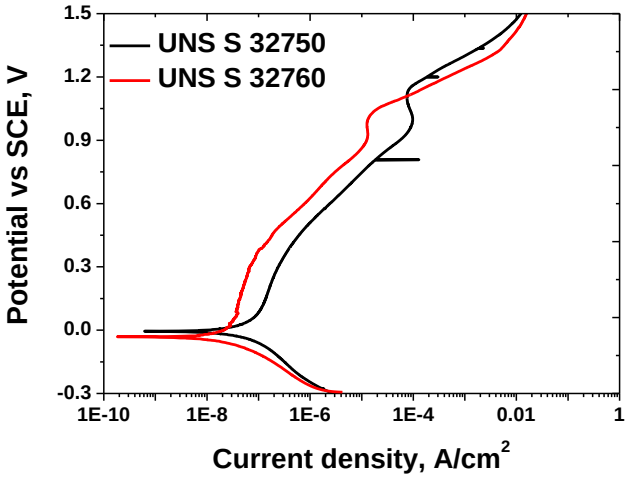

Figure 10. Potentiodynamic polarization curves of UNS S 32750 and UNS S 32760 after solution annealing at 1100 ℃, from −0.3 V to 1.5 V in 3.5 wt. % NaCl.

The corrosion behavior after solution annealing at 1100 °C is shown in Figure 10. The corrosion behavior of SDSS is classified as active polarization, passivation, and pitting potential [9-11, 23]. Table 3 lists the major values for each polarization. UNS S 32750 exhibits a higher E_{corr} but lower I_{corr} than UNS S 32760. Furthermore, UNS S 32750 exhibits a higher pitting potential than UNS S 32760. This is owing to the changes in chemical composition caused by Cu and W.

Table 3. Values of the major points on the potentiodynamic polarization curves of UNS S32750 and UNS S 32760 at 1100 ℃.

Condition	E_{corr}	I_{corr}	Passivation range	E_{pit}
UNS S 32750	–0.097 V	7×10^{-8} A/cm^2	–0.016 V ~ 1.131 V	1.141 V
UNS S 32760	–0.042 V	2×10^{-8} A/cm^2	–0.029 V ~ 1.019 V	1.023 V

Table 4. Values of resistance and CPE obtained for UNS S32750 and UNS S 32760 at 1100 ℃.

Condition	R_s (Ohms)	CPE		R_p (Ohms)
		C	n	
UNS S 32750	6.1	7.77×10^{-5}	0.82	372,240
UNS S 32760	6.0	7.12×10^{-5}	0.81	421,350

Figures 11 and 12 show the Bode and Nyquist plots, respectively, obtained via EIS [13]. The Nyquist plot shows a half cycle. The Bode plot reveals a high phase degree over a frequency range, a linear relationship with a slope close to 1 between IZI and frequency, and a phase decrease near I80°I at low frequencies, highlighting the highly capacitive passivation behavior typical of stainless steel. The

passivation behavior of SDSS is attributable to the considerably low passivation rate, and the equivalent circuit in Figure 13 is fitted to the EIS data to quantify the electrochemical parameters [18].

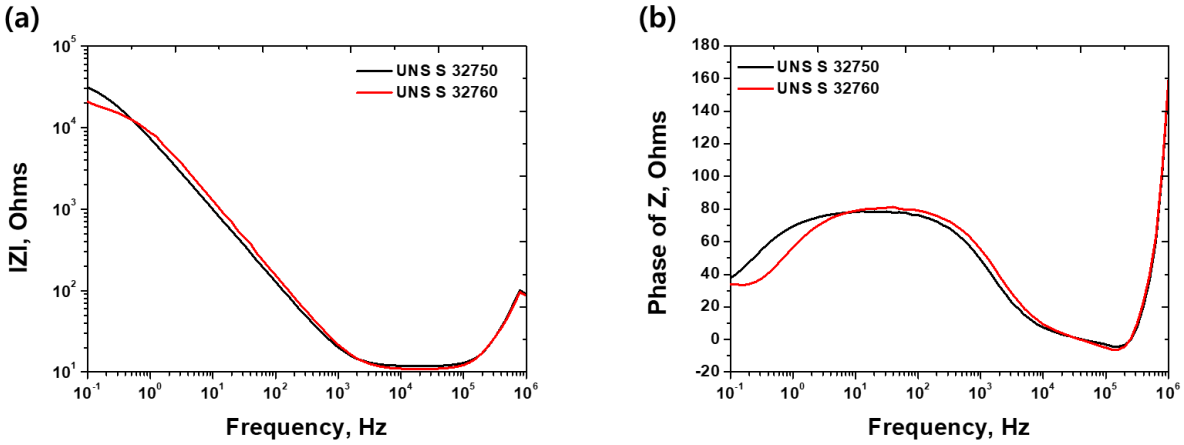

Figure 11. Bode plots of UNS S32750 and UNS S 32760 SDSSs after heat treatment at 1100 ℃ in 3.5 wt. % NaCl: (a) IZI (Ω) as a function of the frequency, and (b) Z (Ω) phase as a function of frequency.

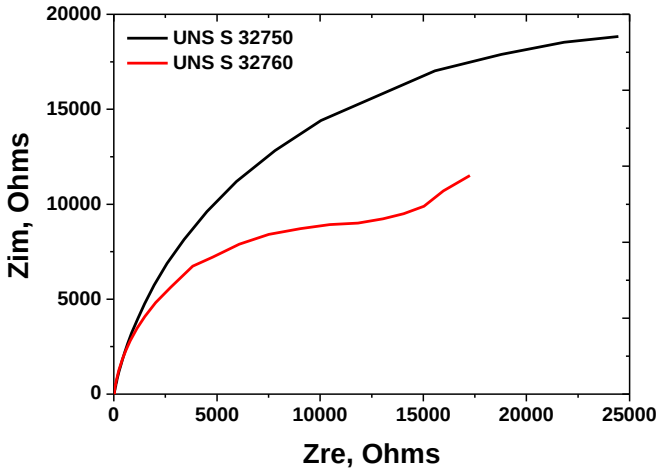

Figure 12. Nyquist plot of the UNS S32750 and UNS S 32760 SDSSs after heat treatment at 1100 ℃ in 3.5 wt. % NaCl.

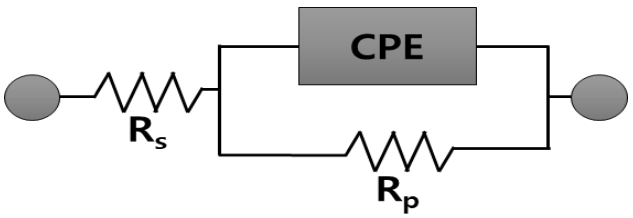

Figure 13. Electrical equivalent circuit used to fit the Bode phase diagrams of the UNS S 32750 and UNS S 32760 SDSSs.

In this equivalent circuit, R_s represents the solution resistance. The constant phase element (CPE) is the double-change layer capacity (C), and the polarization resistance (R_p) is the charge-transfer resistance. The electrochemical impedance parameters obtained by fitting the EIS diagrams are listed in Table 4. The value of n is 0.82, indicating that the passivation film has the same thickness. Although it has an equivalent passivation layer, the corrosion resistance of SDSS varies with the state of the alloy [12, 13].

The corrosion resistance of SDSS varies with the heat-treatment temperature, and the difference in Cu and W contents influences the corrosion resistance. As stabilizing elements of austenite and ferrite, Cu and W, respectively, showed differences in performance. This affects the annealing temperature of the solution.

Changes in Cu and W contents influenced the electrochemical properties; UNS S 32760 heated to 1100 °C exhibited a low reactivity but enhanced the uniform corrosion rate. Moreover, the addition of Cu and W changed the optimal solution annealing temperature; optimal solution annealing (1080 °C for UNS S 32760) induced an increase in the pitting corrosion resistance of the steel.

4. CONCLUSIONS

In this study, the electrochemical properties of UNS S 32750 and UNS S 32760 SDSSs as a function of the heat-treatment temperature were analyzed, and the following conclusions were drawn:

1. UNS S 32760 exhibited a decreased austenite volume fraction upon the addition of Cu and W; however, it exhibited a lower solution heat-treatment temperature than UNS S 32750 because its ferrite fraction increased owing to the addition of W.

2. Although UNS S 32750 and UNS S 32760 exhibited equivalent passivation layers, they exhibited different pitting corrosion resistances. The addition of Cu improved the uniform corrosion resistance and not the pitting corrosion resistance, whereas the addition of W improved the pitting corrosion resistance.

3. SDSS exhibited high corrosion resistance; however, this resistance changed with the heat-treatment temperature. The addition of W decreased the heat-treatment temperature because of the stabilization of the ferrite. Alloys with equivalent PREN also require control of the solution annealing temperature according to the alloy composition.

ACKNOWLEDGMENTS
This study was supported by a National Research Foundation of Korea (NRF) grant (no. 2020R1A5A8018822) funded by the Korean Government (MSIT).

References

1. K. Peter and D. Singamneni, *J. Mater. Res. Technol*, 17 (2022) 601,
2. A. Baghdadchi, V. A. Hosseini, M. A. V. Bermejo, B. Axelsson, E. Harati, M. Ho¨gstro¨m, and L.

Karlsson, *J Mater Sci*, 1 (2022) 19
3. S. A. Policastro, J. M. Shockley, M. J. Strom, C. R. So, D. J. Horton, K. J. Wahl, *Wear*, 494-495 (2022) 204249
4. A. Yarovchuk, A. Dikov, K. Tsay, *J. Phys. Conf. Ser*, 2155 (2022) 012011
5. L. Lei. Y. Sun, K. Zheng, X. Wang, P. He, Y. Liu, Q. Yao, L. Yin, Y. Wan, J. Li, Y. Jiang, *Corros. Sci,* 183, 1 (2021) 109311
6. O. P. Calabokis, Y. N. Rosa, C. M.Lepienski, R. P. Cardoso, P.o C. Borges, *Surf. Coat. Technol*, 413, 15 (2021) 127095
7. P. Renner, Y. Chen, Z. Huang, A. Raut, H. Liang ,*Lubricants,*9 (2021) 52,
8. R. Silva, G. S. Vacchi, C. L. Kugelmeier, I. G. R. Santos, A. A. M. Filho, D. C. C. Magalhães, C. R. M. Afonso, V. L. Sordi, C. A. D. Rovere, *J. Mater. Sci. Technol*, 98 (2022) 123
9. B. Shin, J. Park, J. Jeon, S. Heo, and W. Chung, *Anti-Corros. Methods mater*, 65, 5 (2018) 492
10. D. Cho, J. Park, S. Hong, J. Hwang, S. Kim, *J. Korean Inst. Met. Mater*, 54 (2021) 102
11. B. Shin, D. Kim, S. Park, J. Park, M. Hwang, and W. Chung, *Anti-Corros. Methods mater*., 66, 1 (2019) 61
12. C. J. Park, V. S. Rao, and H. S. Kwon, *Corrosion*, 61 (2005) 76
13. S. Jeon, S. Kim, I. Lee, Y. Park, *Corros. Sci.* 52 (2010) 3537
14. N. Renaudot, E. Chauveau, M. Mantel, *Metall. Ital*, 9 (2012) 29.
15. M. Garibaldi, I. Ashcroft, M. Simonelli, R. Hague, *Acta Mater*, 110 (2016) 207
16. K. Davidson, G. Littlefair,S. Singamneni, *J Manuf Process*, 1-17 (2021)
17. F. Cao, G. Huang, W. Guan, W. Hou, R.Ni, Y. Shen, Q. Liu, *J Manuf Process*, 73 (2022) 611
18. D. Jiang,X.Gao, Y. Zhu, C. Hutchinson, A. Huang, *Mater. Sci. Eng*. A, 833 (2022) 142557
19. Y.S. Ahn and J.P. Kang, *Mater. Sci. Technol*, 16, 4 (2000) 382.
20. F. Khoshnaw, C. Marinescu, A. Sofronia, C. Munteanu, M. Marcu, L. E. Barbulescu, C. Ciobota, E. M. Cojocaru, S. Tanasescu, and A. Paraschiv, *Mater. Today*, 28 (2021) 102644.
21. S. S. M. Tavares, J. M. Pardal, L. F. Noris, and M. G. Diniz, *J. Mater. Res. Technol*., 15 (2021)
22. R. Mondal, S. K. Bonagani, P. Raut, S. Kumar, P. V. Sivaprasad, G. Chai, V. Kain and I. Samajdar, *J. Mater. Eng and Perform.,* (2021) (in press)
23. H. S. Abdo, A. H. Seikh, J. A. Mohammed, T. Uzzaman*, Metals,* 11, 8 (2021) 1205.